Raman Spectroscopy in the Research of Carbon Materials

Kinshuk Dasgupta

Materials Group, Bhabha Atomic Research Centre, Mumbai 400085

Email: kdg@barc.gov.in

Abstract:

Raman spectroscopy has become an indispensable tool in the field of material science, especially in the study of carbon materials. Its non-destructive nature, sensitivity to molecular vibrations, and ability to provide detailed information about the chemical composition, structure, and crystallinity make it a powerful technique for characterizing a wide range of carbon-based materials. This article delves into the significance of Raman spectroscopy in the research of carbon materials, exploring its principles, the types of carbon materials it can analyze, and the key findings it has facilitated.

Keywords: Raman spectroscopy; Carbon materials; Enhanced Raman techniques; Radial breathing mode; Stokes and anti-Stokes scattering

1.   Introduction:

Raman spectroscopy is a vibrational spectroscopic technique based on the inelastic scattering of monochromatic light, usually from a laser source. When light interacts with a material, most photons are elastically scattered (Rayleigh scattering), but a small fraction undergoes inelastic scattering (Raman scattering). This inelastic scattering results in a shift in the energy of the scattered photons, corresponding to the vibrational energies of the molecules in the sample. The Raman spectrum, which plots intensity versus the Raman shift (measured in wavenumbers, cm^{-1}), provides a fingerprint of the material's molecular vibrations.

1.1   Principles of Raman Spectroscopy

Raman spectroscopy relies on the Raman Effect, first observed by C.V. Raman in 1928 [1]. When a photon interacts with a molecule, it can either gain or lose energy, depending on the vibrational state of the molecule. This energy difference between the incident and scattered photons gives rise to the Raman shift. The Raman spectrum thus provides information about the vibrational modes of the molecules in the sample.

The key features of a Raman spectrum include [2]:

Raman Shift (Δv): The difference in wavenumber between the incident and scattered light, typically measured in cm^{-1}.

Intensity: The strength of the Raman signal, which depends on factors such as the concentration of the molecules and the polarizability of the bonds.

Peak Position: The specific wavenumber at which a peak occurs, corresponding to a particular vibrational mode of the molecule.

Peak Width: The broadness of the peak, which can indicate the degree of crystallinity or disorder in the material.

1.2   Theory of Raman Scattering

Raman scattering is an inelastic light scattering phenomenon where the frequency of the scattered light differs from that of the incident light. This frequency shift arises from the interaction of the incident light with molecular vibrations within the sample. When a photon interacts with a molecule, it can either excite a vibrational mode (Stokes scattering) or de-excite an already excited mode (anti-Stokes scattering). Stokes scattering results in a lower-frequency scattered photon, while anti-Stokes scattering produces a higher-frequency photon. The intensity ratio of Stokes and anti-Stokes lines provides valuable information about the vibrational energy levels and temperature of the sample [3]. The schematic of the energy transition is given in **Fig. 1**.

1.3   Working of Raman Spectrometer

A monochromatic light source, usually in the visible or near-infrared region, provides the excitation energy for Raman scattering. The choice of laser wavelength depends on the sample and the desired information. The material to be analysed is placed in the path of the laser beam. Collection optics focus the scattered light from the sample onto the entrance slit of the spectrometer. A filter, such as a notch filter or edge filter, removes the intense Rayleigh scattering from the Raman signal, which is crucial because Raman scattering is typically very weak compared to Rayleigh scattering. The monochromator disperses the Raman scattered light into its constituent wavelengths, typically consisting of a diffraction grating that diffracts the light based on its wavelength, separating the different Raman shifts. A sensitive detector, such as a charge-coupled device (CCD) array detector, records the intensity of the Raman scattered light at each wavelength. The schematic of the Raman spectrometer is given in **Fig.2**.

2.   Carbon Materials and Their Importance

Carbon materials, owing to their unique properties, have become central to various fields, including electronics, energy storage, and nanotechnology. These materials exist in several allotropes, including graphite, diamond, graphene, carbon nanotubes, and fullerenes, each with distinct structures and properties [4].

Graphite: Composed of layers of hexagonally arranged sp^2 hybridized carbon atoms in ABAB…..stacking (**Fig. 3a**), graphite is used in a wide range of applications, from lubricants to electrodes.

Diamond: Known for its hardness and thermal conductivity, diamond is sp3 hybridized FCC structure (**Fig. 3b**) used in cutting tools, optics, and electronics.

Graphene: A single layer of sp^2 hybridized carbon atoms arranged in a hexagonal lattice (**Fig. 3c**), graphene exhibits exceptional electrical, thermal, and mechanical properties.

Carbon Nanotubes (CNTs): Cylindrical nanostructures with sp^2 hybridized carbon atoms (**Fig. 3d**) having remarkable strength, electrical conductivity, and thermal stability.

Fullerenes: Spherical or cage like structure (**Fig. 3e**) composed entirely of carbon, with potential applications in medicine, electronics, and materials science.

3.   Raman Spectroscopy in Carbon Materials

Raman spectroscopy is particularly well-suited for studying carbon materials due to its ability to probe the vibrational modes associated with the sp^2 and sp^3 hybridized carbon atoms. The technique can provide detailed insights into the structure, defects, electronic properties, and interactions of carbon materials.

3.1   Raman Spectroscopy of Graphite and Graphene

Graphite and graphene are among the most studied carbon materials using Raman spectroscopy. The graphene used in this study has been synthesised in-house by CVD method[5]. The graphite were obtained from Tianjin Dingshengxin Chemical Industry Co. Ltd. The Raman spectra were acquired using a 514 nm diode laser with an acquisition time of 1 second and a power of 20 mW. These parameters were consistently used for obtaining the spectra of other carbon nanomaterials analyzed in this study. Few mg of sample was spread on a glass slide and spectrum was acquired. The Raman spectrum (refer **Fig. 4**) of these materials is characterized by several key features [6]:

G Band: The G band, observed around 1580 cm^{-1}, corresponds to the in-plane vibrational mode (E_{2g}) of sp^2 carbon atoms. It is present in all sp^2 carbon systems and is a signature of graphitic materials.

D Band: The D band, appearing around 1350 cm^{-1}, is associated with the presence of defects or disorder in the sp^2 carbon lattice. It arises due to the breathing modes of sp^2 rings and is activated by defects such as edges or vacancies in the lattice. The intensity ratio of the D to G band (I_D/I_G) is often used as a measure of the degree of disorder in the material.

2D Band: The 2D band, also known as the G' band, is a second-order overtone of the D band, observed around 2700 cm^{-1}. In graphene, the 2D band is particularly important as it provides information about the number of layers and the stacking order of the graphene sheets. In single-layer graphene, the 2D band is a sharp, single peak, whereas in multi-layer graphene, it splits into multiple components.

D' Band: The D' band, appearing around 1620 cm^{-1}, is another defect-related peak, often observed in conjunction with the D band. The intensity of the D' band, along with the D and G bands, can provide insights into the nature and concentration of defects in the material.

D" Band: The D" mode is a higher-order overtone or combination. It typically appears at higher wavenumbers compared to the D band and is indicative of more complex vibrational interactions within the material. The presence and intensity of the D" band can provide insights into the material's structural properties and defect levels.

D+D" Peak: The D+D″ peak is observed around 2425 cm^{-1}, results from simultaneous interactions involving both the D and D″ phonons. This peak is particularly intense in disordered graphene materials and serves as an indicator of the material's quality and structural characteristics.

In graphite with small defect concentration additional peaks like D+D′ also appear.

Raman spectroscopy has been instrumental in characterizing graphene's properties, such as layer number, quality, and the effects of strain or doping. For instance, the 2D band analysis allows researchers to distinguish between single-layer and multi-layer graphene, while the D band intensity reveals information about defects or functionalization.

3.2   Raman Spectroscopy of Carbon Nanotubes

Carbon nanotubes (CNTs) exhibit a rich and complex Raman spectra, reflecting their unique structures and electronic properties. Single –walled CNT (SWCNT) and multi-walled CNT (MWCNT) show different features [7]. CNTs used in this study were synthesized in-house by FC-CVD method [8-10].

Single-walled carbon nanotubes (SWCNTs) are one of the most fascinating nanomaterials, renowned for their unique structural, electrical, and mechanical properties. Raman spectroscopy plays a critical role in characterizing these properties, providing insights into the diameter, chirality, electronic structure, and defect density of SWCNTs. The Raman spectrum of SWCNTs is rich with information and can be analyzed by focusing on several key features: the radial breathing mode (RBM), the G-band, the D-band, and the 2D-band [11].

Radial Breathing Mode (RBM): The radial breathing mode (RBM) is one of the most characteristic and important features in the Raman spectrum of SWCNTs. It is a low-frequency mode, typically observed in the range of 100-300 cm^{-1}, and corresponds to the coherent radial expansion and contraction of the nanotube. The frequency of the RBM (ω_{RBM}) is inversely proportional to the nanotube diameter (d), and can be expressed approximately by the following empirical relation [12]:

$$\omega_{RBM} = C_1/d + C_2$$

where C_1 and C_2 are constants that depend on the environment and nanotube characteristics. This mode is particularly useful because it allows researchers to determine the diameter of the SWCNTs directly from the Raman spectrum. **Fig. 5 (a-d)** shows how after capturing RBM mode from different positions of a SWCNT bundle we can get diameter distribution.

The RBM is sensitive to the environment surrounding the nanotubes. For example, if the nanotube is in a bundle or interacting with a substrate, the RBM frequency may shift. Additionally, the intensity of the RBM is linked to the resonance condition between the incident laser energy and the electronic transition energy of the SWCNT, which provides information on the electronic structure of the nanotube.

G-Band: The G-band is another critical feature in the Raman spectrum of SWCNTs. It is typically observed around 1580 cm^{-1} and arises from the in-plane stretching vibrations of carbon-carbon bonds in the sp^2 hybridized carbon atoms. Unlike graphene or graphite, where the G-band appears as a single peak, the G-band in SWCNTs is split into two components: G+ and G- (**Fig. 6**).

The G+ band corresponds to the longitudinal optical (LO) phonon mode, which involves vibrations along the axis of the nanotube. It is usually located at a higher frequency (~1590 cm^{-1}) and is relatively sharp.

The G- band corresponds to the transverse optical (TO) phonon mode, which involves vibrations perpendicular to the nanotube axis. It appears at a lower frequency (~1560-1570 cm^{-1}) and is broader than the G+ band.

The splitting of the G-band is particularly important because it can be used to distinguish between metallic and semiconducting SWCNTs. In semiconducting SWCNTs, the G- band is narrow and well-defined, while in metallic SWCNTs, it is broader and lower in frequency. This difference is due to the electron-phonon coupling, which is stronger in metallic nanotubes.

The study of anti-Stokes Raman spectra of single-walled carbon nanotubes reveals significant asymmetries compared to Stokes spectra, attributed to unique resonant enhancement phenomena influenced by their one-dimensional electronic density of states, which allows for selective identification of different nanotube types under specific laser excitation conditions [13].

D-Band: The D-band, typically observed around 1350 cm^{-1}, is associated with the presence of defects or disorder in the SWCNT structure. It arises from the breathing modes of sp^2 carbon atoms in rings and is activated by the presence of defects, such as vacancies, impurities, or functional groups that break the symmetry of the carbon lattice.

The intensity ratio of the D-band to the G-band (I_D/I_G) is often used as a measure of the defect density in SWCNTs. A higher I_D/I_G ratio indicates a greater degree of disorder or a higher concentration of defects. This ratio is particularly useful for evaluating the quality of SWCNTs, especially after processes like functionalization or chemical treatment.

2D-Band (G'-Band): The 2D-band, also known as the G'-band, is a second-order overtone of the D-band and is typically observed around 2600-2700 cm^{-1}. Unlike the D-band, the 2D-band does not require the presence of defects for activation and is always present in the Raman spectrum of SWCNTs.

The 2D-band provides additional information about the electronic structure of the SWCNTs. Its shape, position, and intensity can vary depending on the number of layers, the presence of strain, and the electronic properties of the nanotubes. In SWCNTs, the 2D-band is usually sharp and symmetric, and its intensity is strongly dependent on the resonance condition with the incident laser energy.

Multi-walled carbon nanotubes (MWCNTs) consist of multiple concentric single-walled carbon nanotubes (SWCNTs), with each layer having a different diameter and possibly different chirality. The Raman spectrum of MWCNTs shares many features with that of SWCNTs, but the additional layers and the complex interactions between them lead to some

distinct characteristics. The RBM peak in MWCNT is generally missing and the splitting of the G band in MWCNT is not witnessed in MWCNT unlike SWCNT as the combined effect of multiple tubes in the MWCNT nullifies the effect (**Fig. 7**). The Raman spectrum of double-walled carbon nanotubes (DWCNT) is characterized by distinct peaks such as the radial breathing mode (RBM), D band, and G band, where the RBM frequency is sensitive to the inner and outer tube diameters; in contrast, multi-walled carbon nanotubes (MWCNT) typically show broader peaks and a more complex spectral profile due to multiple concentric layers, leading to overlapping signals that complicate the interpretation of individual modes [14]

3.3   Raman Spectroscopy of Diamond

Diamond, with its purely sp^3 carbon bonding, exhibits a characteristic Raman peak at 1332 cm^{-1}, corresponding to the stretching of the carbon-carbon bonds in the diamond lattice. Diamond used in this study is diamond powder used in polishing industry [15]. The sharpness and position of this peak are indicative of the diamond's purity and crystallinity. Raman spectroscopy is widely used to assess the quality of synthetic diamonds, identify defects, and study phase transitions, such as the conversion of diamond to graphite under high temperatures or pressures[16].

In addition to pure diamond, Raman spectroscopy is also employed to study diamond-like carbon (DLC) films (**Fig. 8**), which are amorphous carbon materials with a mixture of sp^2 and sp^3 bonding. The Raman spectrum of DLC typically shows broad peaks around 1350 cm^{-1} (D band) and 1550 cm^{-1} (G band), similar to those of disordered graphite, but with differences in peak position and intensity that reflect the sp^2/sp^3 ratio and the degree of disorder.

3.4   Raman Spectroscopy of Fullerenes

Fullerenes, such as C60 and C70, are spherical carbon molecules with unique electronic and vibrational properties [17]. The Raman spectra of fullerenes are characterized by several distinct peaks corresponding to the vibrational modes of the carbon atoms in the cage structure. For example, the Ag(2) mode of C60, observed around 1469 cm^{-1}, is a prominent feature in its Raman spectrum (**Fig. 9**).

Raman spectroscopy has been crucial in studying the structural and electronic properties of fullerenes, as well as their interactions with other materials. For instance, the shifts in Raman peaks can provide information about the charge transfer between fullerenes and dopant molecules, which is important in understanding their behaviour in organic photovoltaics and other electronic applications.

3.5   Effect of Excitation Wavelength

The intensity of Raman scattering is inversely proportional to the fourth power of the laser wavelength. This means that longer wavelengths (e.g., near-infrared) produce weaker Raman signals compared to shorter wavelengths (e.g., UV or visible light). For instance, using a near-infrared laser can result in spectra that are up to 15 times less intense than those obtained with a UV laser under identical conditions.

Resonance Enhancement: The choice of laser wavelength can also affect resonance conditions, which enhance specific spectral features. For example, certain phonon populations in carbon materials may resonate differently depending on the excitation wavelength, leading to shifts in the D band frequency. This resonance effect is crucial for accurately interpreting the microstructure of materials like graphite and carbon nanotubes.

4.   Enhanced Raman Spectroscopic Techniques

4.1   Surface-enhanced Raman Spectroscopy

Surface-enhanced Raman spectroscopy (SERS) is a powerful analytical technique used to enhance the Raman signals of carbon materials by leveraging plasmonic effects from metallic nanostructures, such as silver or gold nanoparticles [18]. This method is particularly effective for detecting low-concentration analytes, revealing subtle structural features, and identifying functional groups in carbon-based materials. SERS enables high sensitivity and specificity, making it an invaluable tool for studying carbon nanomaterials, such as graphene, carbon nanotubes, and amorphous carbon, in various applications ranging from sensing to catalysis.

4.2   Tip-enhanced Raman Spectroscopy

Another area of ongoing research is the development of tip-enhanced Raman spectroscopy (TERS), which combines the spatial resolution of atomic force microscopy (AFM) with the chemical sensitivity of Raman spectroscopy [19]. It utilizes a sharp metallic tip, often coated with a noble metal like gold or silver, to enhance the Raman signal from molecules located at the tip apex. TERS has the potential to provide nanoscale insights into carbon materials, enabling the study of local variations in structure and composition that are not accessible with conventional Raman spectroscopy.

TERS allows for highly localized Raman scattering measurements on carbon materials. By using a sharp metal tip to concentrate the incident laser light, TERS provides nanoscale spatial resolution, enabling the characterization of individual carbon nanotubes, graphene layers, and

defects within these materials [20]. This technique has proven valuable in understanding the structure, properties, and electronic behavior of carbon-based nanomaterials.

5.   Applications of Raman Spectroscopy in Carbon Material Research

Raman spectroscopy has been applied to a wide range of studies involving carbon materials, contributing to advancements in various fields. Some of the key applications include:

5.1   Characterization of Graphene-Based Materials: Raman spectroscopy is widely used to characterize graphene and its derivatives, such as graphene oxide (GO) and reduced graphene oxide (rGO). The technique provides insights into the number of layers, degree of oxidation, and reduction efficiency, which are critical for tailoring the properties of graphene-based materials for specific applications. To determine the number of layers in graphene oxide using Raman spectroscopy, one can analyze the intensity ratio of the 2D band to the G band (I_{2D}/I_G), as well as observe the peak positions and shapes, where a higher ratio typically indicates fewer layers and a broader 2D peak suggests an increase in layer number [21]. The correlation between the full width at half maximum (FWHM) of the Raman 2D peak and the number of graphene layers indicates that as the number of layers increases, the FWHM generally decreases, with single-layer graphene exhibiting a FWHM of approximately 28.7 cm^{-1} and multilayer graphene showing broader peaks due to interlayer interactions and disorder [22]. Raman spectroscopy is a powerful tool for differentiating between GO and reduced rGO by analyzing the intensity ratios and positions of specific peaks, particularly the D, G, and D' bands; for instance, the energy difference between the D' and G peaks can quantitatively define the degree of reduction, where a negative difference indicates GO, a small positive difference indicates rGO, and a larger positive difference indicates pristine graphene [23].

5.2   Quality Control of Carbon Nanotubes: The synthesis of high-quality CNTs is challenging, and Raman spectroscopy serves as a valuable tool for quality control. By analyzing the RBM, G, and D bands, researchers can assess the purity, diameter distribution, and defect density of CNTs, ensuring their suitability for applications in electronics, composites, and energy storage. To quantify the amorphous content in carbon nanotubes (CNTs) using Raman spectroscopy, one can analyze the intensity ratios of the D-band and G-band, specifically the I_D/I_G ratio, where a higher ratio indicates a greater presence of amorphous carbon due to increased disorder in the structure. This method effectively distinguishes between crystalline and amorphous phases in carbon materials [24].

5.3   Studying Defects and Functionalization: Defects and functional groups play a crucial role in determining the properties of carbon materials. Raman spectroscopy is highly sensitive to these features, making it an ideal technique for studying the effects of defects, doping, and functionalization on the material's properties. For example, in graphene, the I_D/I_G ratio provides a measure of the defect density, while in CNTs, the appearance of new peaks in the Raman spectrum can indicate successful functionalization.

5.4   In-Situ and Operando Studies: Raman spectroscopy can be performed in-situ, allowing researchers to monitor changes in carbon materials under various conditions, such as temperature, pressure, or chemical environment. This capability is particularly useful for studying the behaviour of carbon materials in real-time, such as during the electrochemical cycling of batteries or the growth of graphene by chemical vapour deposition (CVD).

5.5   Nanotechnology and Device Fabrication: Raman spectroscopy is employed in the fabrication and characterization of carbon-based nanodevices, such as graphene transistors and CNT-based sensors. The technique provides valuable information about the structural and electronic properties of the materials, enabling the optimization of device performance.

6.   Challenges and Future Directions

While Raman spectroscopy has proven to be an invaluable tool in carbon material research, it is not without its challenges. One of the primary challenges is the interpretation of complex spectra, especially in materials with a high degree of disorder or in heterogeneous systems. Advanced data analysis techniques, such as multivariate analysis and machine learning, are being developed to address these challenges and extract more detailed information from Raman spectra.

7. Conclusions

Raman spectroscopy has become an essential technique in the research of carbon materials, providing detailed insights into their structure, properties, and behaviour. From the characterization of graphene and CNTs to the study of diamond and fullerenes, Raman spectroscopy has played a pivotal role in advancing our understanding of carbon-based materials and enabling their applications in various fields. As the field of material science

continues to evolve, Raman spectroscopy will undoubtedly remain a key tool for exploring the fascinating world of carbon materials, driving innovation and discovery in the years to come.

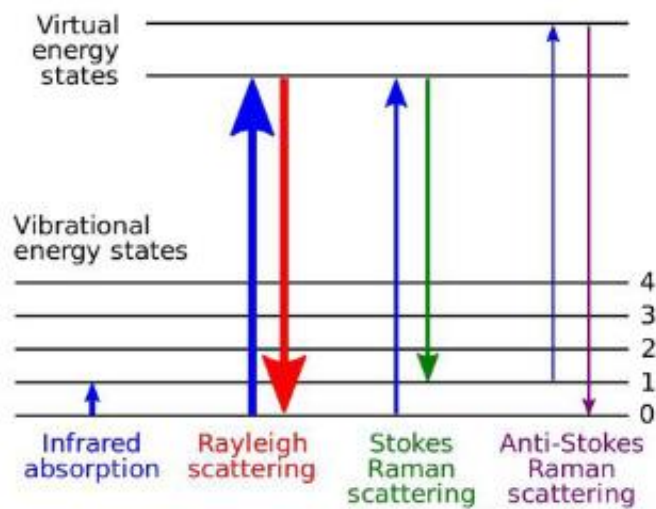**Acknowledgement:**

Figures:

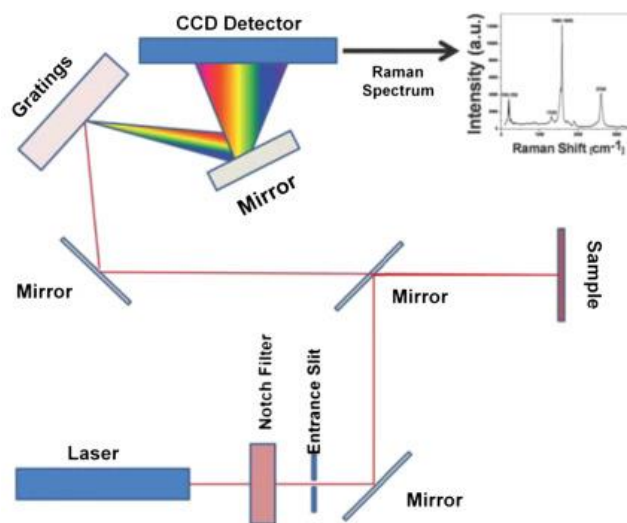**Fig. 1: Energy transition in Rayleigh, Stokes, anti-Stokes scattering [25]**

Fig. 2: Schematic of Raman spectrometer [26]
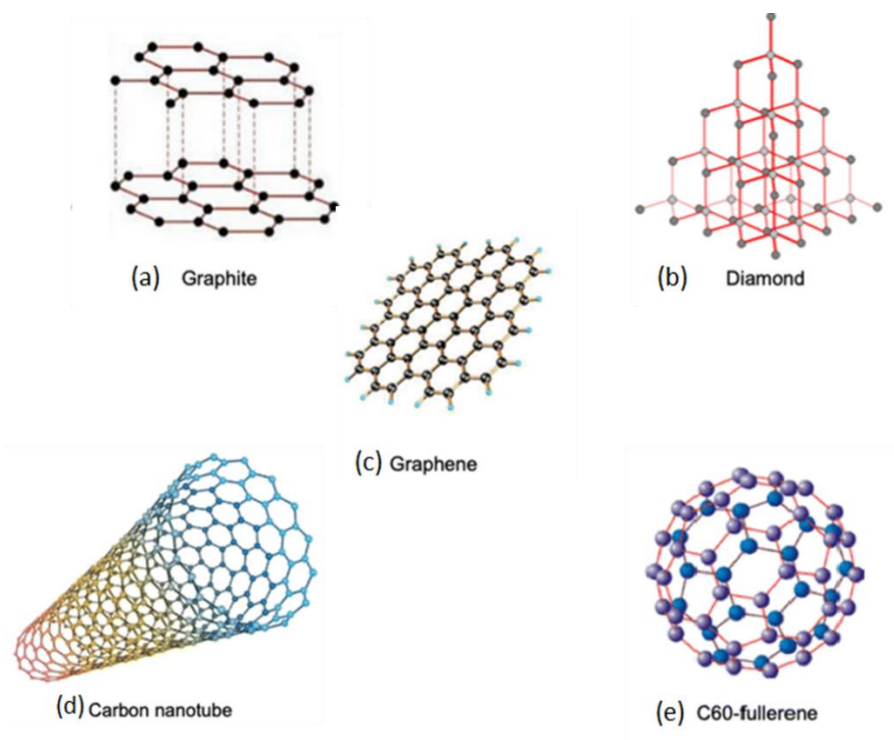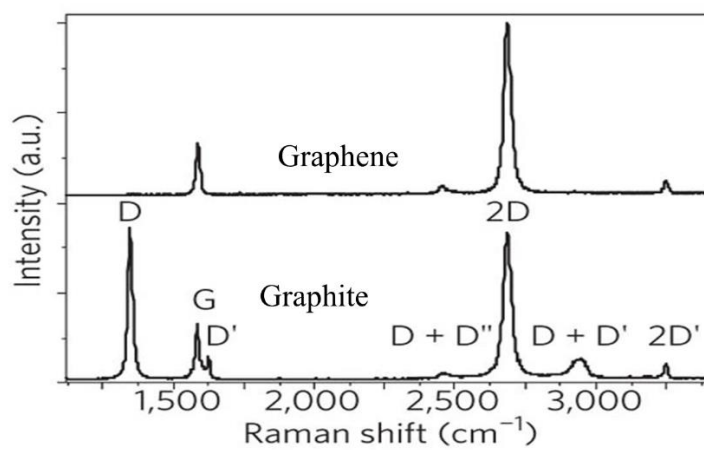
Fig. 3 (a-e): Different structure of carbon [27]
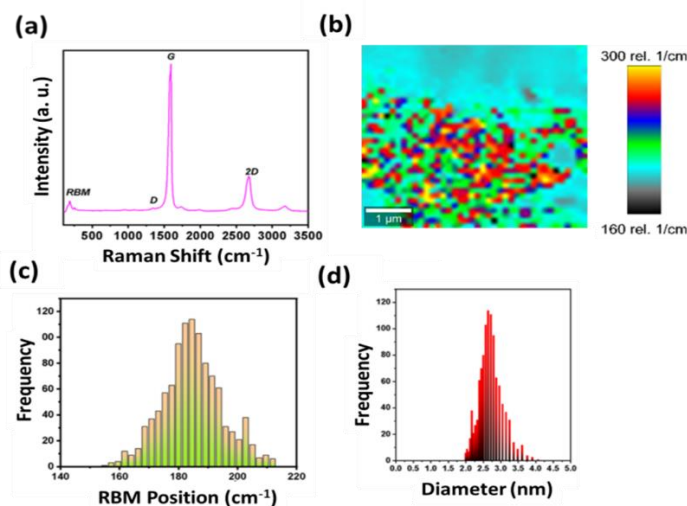

Fig. 4: Raman spectra of graphene and graphite [28]

Fig. 5: (a) Raman spectra of SWCNT, (b) RBM peak mapping in SWCNT in SWCNT bundle, (c) distribution of RBM peak position, and (d) diameter distribution of SWCNT determined from RBM position [11]
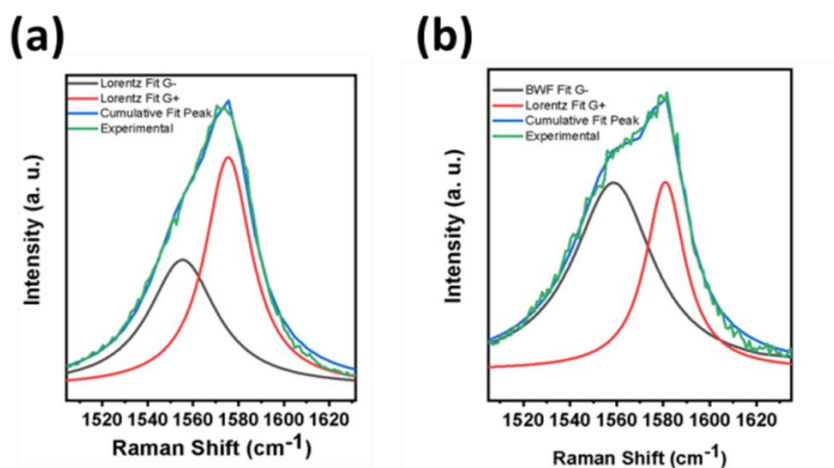

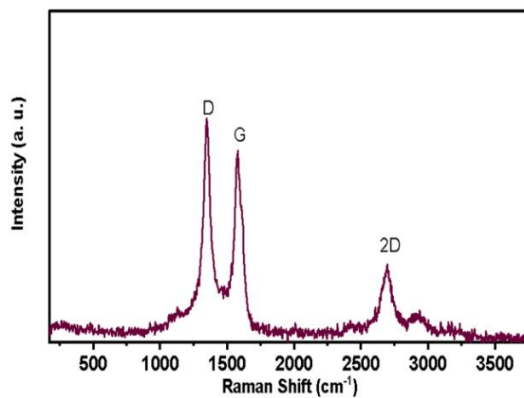**Fig. 6: (a) Deconvolution of G band of metallic SWCNT, and (b) deconvolution of G band of semiconductor SWCNT [11]**
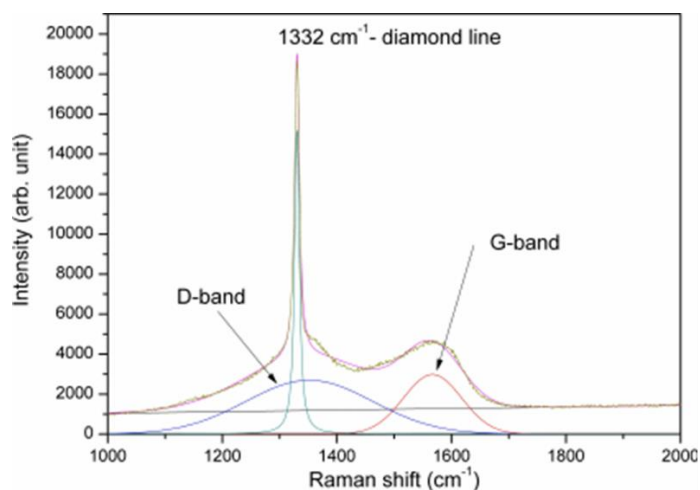
Fig. 7: Raman spectrum of MWCNT [11]

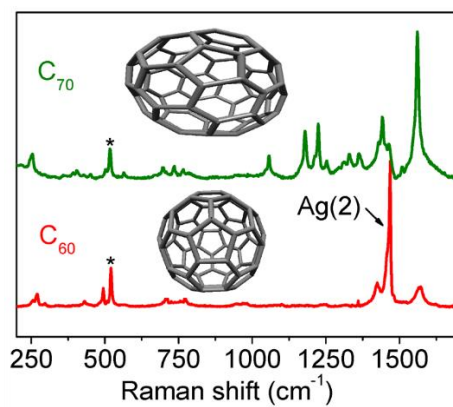**Fig. 8: Raman spectrum from diamond and DLC [29]**

Fig. 9. Raman spectra from C60 and C70 fullerenes

References:

1. C. V. Raman, Indian Journal of physics 2, 387,1928.

2. D. Long, Chichester and New York: Wiley, 2002.

3. B. Schrader, Infrared and Raman spectroscopy: methods and applications, John Wiley & Sons, 2008.

4. K. Dasgupta and D. Sathiyamoorthy, Materials science and technology, 19, 995,2003

5. M. D. Yadav, K. Dasgupta, A. Kushwaha, A. P. Srivastava, A. W. Patwardhan, D. Srivastava and J. B. Joshi, Materials Letters, 199, 180, 2017.

6. A. C. Ferrari, Solid state communications, 143, 47, 2007.

7. M. S. Dresselhaus, A. Jorio, M. Hofmann, G. Dresselhaus and R. Saito, Nano Letters, 10, 751 2010,

8. A. Kaushal, R. Alexander, M. Joshi, J. Singh and K. Dasgupta, Chemical Engineering Journal, 484, 149254, 2024.

9. R. Alexander, A. Kaushal, S. Acharya, J. Prakash, J. Bahadur and K. Dasgupta, Chemical Engineering Journal, 503, 158460, 2025.

10. R. Alexander, A. Khausal, J. Bahadur and K. Dasgupta, Carbon Trends, 9, 100211, 2022.

11. R. Alexander, J. Prakash, A. Kaushal and K. Dasgupta, Phys News, 50, 28. 2020.

12. P. T. Araujo, I. O. Maciel, P. B. C. Pesce, M. A. Pimenta, S. K. Doorn, H. Qian, A. Hartschuh, M. Steiner, L. Grigorian, K. Hata and A. Jorio, Physical Review B, 77, 241403, 2008.

13. S. D. M. Brown, P. Corio, A. Marucci, M. S. Dresselhaus, M. A. Pimenta and K. Kneipp, Physical Review B, 61, R5137, 2000.

14. A. Jorio and R. Saito, Journal of Applied Physics, 129, 021102, 2021.

15. R. Alexander, K. V. Ravikanth, M. R. Gonal, A. P. Srivastava and K. Dasgupta, SN Applied Sciences, 2, 835, 2020.

16. S. Prawer and R. J. Nemanich, Philosophical Transactions of the Royal Society of London. Series A: Mathematical, Physical and Engineering Sciences, 362, 2537, 2004.

17. M. Dresselhaus and P. Eklund, Advances in physics, 49, 705, 2000.

18. E. Le Ru and P. Etchegoin, Principles of Surface-Enhanced Raman Spectroscopy: and related plasmonic effects, Elsevier, 2008.

19. B. Pettinger, P. Schambach, C. J. Villagómez and N. Scott, Annual review of physical chemistry, 63, 379, 2012.

20. G. G. Hoffmann, M. Ghislandia and G. de Witha, Nanotechnology, 18, 315502, 2007.

21. V. Kumar, A. Kumar, D.-J. Lee and S.-S. Park, Materials, 14, 4590, 2021.

22. Z. Lin, X. Ye, J. Han, Q. Chen, P. Fan, H. Zhang, D. Xie, H. Zhu and M. Zhong, Scientific Reports, 5, 11662,2015.

23. A. A. K. King, B. R. Davies, N. Noorbehesht, P. Newman, T. L. Church, A. T. Harris, J. M. Razal and A. I. Minett, Scientific Reports, 6, 19491, 2016.

24. S. I. Moseenkov, V. L. Kuznetsov, N. A. Zolotarev, B. A. Kolesov, I. P. Prosvirin, A. V. Ishchenko and A. V. Zavorin, Materials, 16, 1112, 2023.

25. T. Subramaniam and R. Premanand, J Laser Opt Photonics, 5, 1000189, 2018.

26. N. John and S. George, in Spectroscopic Methods for Nanomaterials Characterization, eds. S. Thomas, R. Thomas, A. K. Zachariah and R. K. Mishra, Elsevier, pp. 95-127, 2017.

27. A. Aligayev, F. Raziq, U. Jabbarli, N. Rzayev and L. Qiao, in Graphene, Nanotubes and Quantum Dots-Based Nanotechnology, ed. Y. Al-Douri, Woodhead Publishing, pp. 355-420, 2022.

28. A. C. Ferrari and D. M. Basko, Nature Nanotechnology, 8, 235, 2013.

29. A. Dychalska, P. Popielarski, W. Franków, K. Fabisiak, K. Paprocki and M. Szybowicz, Materials Science-Poland, 33, 799, 2015.